A constraint Jacobian based approach for static analysis of pantograph masts

B. P. Nagaraj*, R. Pandiyan†
ISRO Satellite Centre,
Bangalore, 560 017, India
and
Ashitava Ghosal‡
Dept. of Mechanical Engineering,
Indian Institute of Science,
Bangalore 560 012, India.
Fax.: +91 80 2360 0648

Abstract

This paper presents a constraint Jacobian matrix based approach to obtain the stiffness matrix of widely used deployable pantograph masts with scissor like elements (SLE). The stiffness matrix is obtained in symbolic form and the results obtained agree with those obtained with the force and displacement methods available in literature. Additional advantages of this approach are that the mobility of a mast can be evaluated, redundant links and joints in the mast can be identified and practical masts with revolute joints can be analysed. Simulations for a hexagonal mast and an assembly with four hexagonal masts is presented as illustrations.

Keywords: Pantograph masts, Deployable structures, Null-space, Jacobian, Stiffness matrix

1 Introduction

Deployable structures can be stored in a compact configuration and are designed to expand into stable structures capable of carrying loads after deployment. In their general form,

*Spacecraft Mechanisms Group
†Flight Dynamics Group
‡Corresponding author. email: asitava@mecheng.iisc.ernet.in

they are made up of a large number of straight bars (links) connected by revolute joints and with one or more cables used for deployment or increasing the stiffness of the deployed structure (see, for example, [1]-[2]). Initially, the whole assembly of bars can be stowed in a compact manner and, when required, can be unfolded into a predefined large-span, load bearing structural form by simple actuation of one or more cables. This characteristic feature makes them eminently suitable for a wide spectrum of applications, ranging from temporary structures that can be used for various purpose in ground to the large structures in aerospace industry. Deployable/collapsible mast are often used for space applications since in their collapsed form they can be easily carried as a spacecraft payload and expanded in orbit to a desired size. Many deployable systems use the pantograph mechanism or scissor-like elements (SLE's). Typically, an SLE has a pair of equal length bars connected to each other at an intermediate point with a revolute joint. The joint allows the bars to rotate freely about an axis perpendicular to their common plane. Several SLE's are connected to each other in order to form units which in plan view appear as regular polygons with their sides and radii being the SLE's. Several such polygons, in turn, are linked in appropriate arrangements leading to deployable structures that are either flat or curved in their final deployed configurations. The assembly is a mechanism with one degree of freedom from the stowed/folded configuration till the end of deployment. The deployment is through an active cable and after deployment the assembly is a pre-tensioned structure. Active cables control the deployment and pre-stress the pantograph and passive cables are pre-tensioned in the fully deployed configuration. These cables have the function of increasing the stiffness in the fully deployed configuration [3].

1.1 Kinematics and mobility

The kinematics of multi-body mechanical systems can be studied by use of relative co-ordinates [4], reference point coordinates as used in the commercial software ADAMS [5]

or Cartesian coordinates (also called natural/basic coordinates) [6]. In references [7], [8], Garcia and co-workers have used Cartesian coordinates to obtain the constraints equations for different types of joints and for kinematic analysis of mechanisms. Typical pantograph masts are over-constrained mechanisms according to Grübler-Kutzbach criteria, and in reference [9], Cartesian coordinates have been used to study the kinematics and mobility of deployable pantograph masts – the authors use the derivative of the constraint equations and develop an algorithm to obtain redundant link and joints in over-constrained deployable masts, perform kinematic analysis and obtain global degrees of freedom. The key advantage of Cartesian coordinates is that the constraint equations are *quadratic* (as opposed to transcendental equations for relative coordinates), and, hence their derivatives are *linear*. As shown in [9], these features allows easier manipulation and simplification of expressions in a computer algebra system to obtain symbolic expressions and closed-form solutions for the kinematics of pantograph masts. A disadvantage of Cartesian coordinates is that the number of variables is typically larger and tends to be (on average) in between relative coordinates and reference point coordinates. However, for analysis of pantograph masts, the number is not too large and could be handled without much difficulty in the computer algebra system, *Mathematica*, used in this work.

The masts in their deployed configuration become pre-tensioned structures. For pre-stressed structures with pin jointed bars, the necessary condition for the structure to be statically and kinematically determinate is given by the *Maxwell's rule*

$$3j - b - c = 0 \tag{1}$$

where, j is the number of joints, b is the number of bars or links and c is the number of kinematic constraints. Calladine [10] generalized the *Maxwell's rule* as

$$
\begin{aligned}
s &= b - r \\
m &= 3j - c - r \\
3j - b - c &= m - s
\end{aligned} \tag{2}
$$

where, m is the number of internal mechanisms, s is the number of states of self stress, and r is the rank of the equilibrium matrix. This equation is referred to as the *extended Maxwell's rule*. The values m and s depends on the number of bars and joints, topology of the connection and on the geometry of the frame work. The numerical values of the vectors describing s and m, for a given system, can be determined from the singular value decomposition (SVD) of the equilibrium matrix. The concept of using a Jacobian matrix to evaluate the mobility was first presented by Freudenstein [11] for an over-constrained mechanism. Later, the first and higher order derivatives of constraint equations has been used for under constrained structural systems to evaluate mobility and state of self-stress by Kuznetsov [12, 13]

1.2 Structural matrix

The mechanism at the end of deployment becomes a pre-tensioned structure and the structural matrices are useful for evaluating the stiffness/displacement of the SLE masts in the deployed configuration. In literature, researchers have used various methods for formulating the structural matrix for an SLE. These are termed as *force method* [14], *displacement method* [15] and *equivalent continuum model* [16]. We describe each of these methods in brief below.

Force method: In the force method, as used by Kwan and Pellegrino [14], the SLE is discretised into four beam elements. The equilibrium, compatability and flexibility matrices are derived for a typical beam element in a local coordinate system using shear force and

bending moment relationships. These equations are transformed to the global coordinate system by using the rotation matrices and are assembled for the four beam elements, which make up the SLE. The equilibrium matrix is reduced in size by matrix partitioning and by setting the end moments to zero [18]. In this approach one can evaluate the number of self-stress states and the number of infinitesimal mechanisms of the given system by using singular value decomposition (SVD) of the equilibrium matrix [19].

Displacement method: The displacement method is used by Shan [15] to formulate stiffness matrix for the SLE. In his approach, each link of the SLE is called an *uniplet*. One uniplet of the SLE is modeled as an assembly of two beam elements with mid node at the pivot point of SLE. The stiffness matrix was partitioned to have the translation terms and rotational terms in order. The final reduced stiffness matrix is obtained by condensing and removing the rotational degrees of freedom of all the three nodes. In the reference [20], the authors have formulated the stiffness matrix for two uniplets, called as a *duplet*, by using the stiffness matrix of the uniplet developed above. Matrix partitioning is used to get the reduced stiffness matrix which condenses the translational degrees of freedom of the pivot node.

Equivalent continuum model: This approach was used to predict the stiffness characteristics of deployable flat slabs when they are subjected to normal loads [16, 17]. In this method, the SLE is considered as an *equivalent* uniform beams that deflects identically to the given loading as that of an SLE. The flat large deployable structure is substituted with an equivalent grid of uniform beams running in particular directions The beams are rigidly connected to each other. This arrangement is reduced to an equivalent orthotropic plate of constant thickness and stiffness matrix is obtained. The results predicted by this method are approximate unlike above methods and hence can only be used for initial design phase which reduces the computational time. In an exact finite element modeling the storage space requirements are large for large number of SLE units due to the complicated pivotal

connections and hinged connections that require more than one nodal point to be described accurately. The equivalent approach can significantly reduce the computational effort during preliminary design stage.

Comparison of existing methods: The force method gives the additional information about the states of self stress and infinitesimal mechanisms. The displacement method or equivalent continuum model does not give this information. The force method uses two matrix reductions which reduces the matrix of dimension 18×14 to 12×8 in the first step. Further in the second step the matrix dimension is reduced from 12×8 to 10×6, to obtain the final reduced equilibrium matrix. The displacement method has a stiffness matrix of dimension 18×18 for the two assembled beam elements with six degrees of freedom at each node. By condensing the rotational degrees of freedom at all the nodes the matrix dimension reduces to 9×9. The reduced matrix has only translational degrees of freedom at each node. The equivalent continuum approach is useful for very large repetitive structures. However, this method does not give the accurate results when compared to other two methods and, hence, can be used only for initial design phase to reduce computational time.

As mentioned earlier, at the end of deployment we get a structure capable of bearing loads, and in this paper, we extend the approach in [9] to the static analysis of deployable pantograph masts. We present a new approach to formulate the structural matrices for a typical SLE using Cartesian coordinates, the kinematic equations of the SLE/pantograph element, and the constraint Jacobian matrix. These matrices are derived by using the symbolic computation software Mathematica [21]. The results of formulations obtained by this approach matches exactly with the results of force and displacement based methods. Our approach has the advantages of the force method in evaluating the states of self-stress and infinitesimal mechanisms. However, in our approach, the final reduced equilibrium matrix can be obtained in a single step unlike in the force and displacement methods. In addition, the constraint equations of the links and joints are useful in studying the kinematics behavior

of pantograph masts during deployment, in evaluating the redundancy in the links/joints of these over-constrained systems, and in obtaining the final degrees of freedom of the deployable masts. In literature the successive SLE joint connection are assumed to be spherical joints. In a practical pantograph mast, two revolute joints with intersecting axis are used. In this work, we have used the revolute joint constraints for the SLE connected to the successive SLEs by revolute joints.

This paper is organized as follows: In section 2, we present a brief description of the deployable masts considered for the analysis. and present the constraint equations for the links, joints and the SLE with the Jacobian matrix. In section 3, we present the mathematical approach for the evaluation of stiffness matrix for the SLE and the detailed equations are presented in an Appendix. In section 4, we present the stiffness matrix for the cables used in pantograph masts. In section 5, we present the additional constraints and the stiffness matrix due to revolute joints. In section 6, we illustrate our approach by using a planar stacked mast and three dimensional SLE based masts. Finally, in section 7, we present the conclusions.

2 Kinematic description of the SLE masts

In this section a brief description of the SLE masts and formulation of the constraint equations are presented for the sake of completeness (see, [9], for details). In the next section, we use these equations to derive stiffness matrices.

The simplest planar SLE is shown in figure 1. The revolute joint in the middle connects the two links of equal length. The assembly has one degree of freedom. Figure 2 shows a two dimensional stacked SLE mast [3]. This consists of four SLEs stacked one above the other. The deployment angle β can vary continuously from $\beta = 0°$, when the assembly is fully folded, i.e. lying flat on its base and all links are collinear, to $\beta = 45°$ which corresponds to the fully deployed configuration. This has eight passive cables connecting the adjacent joints

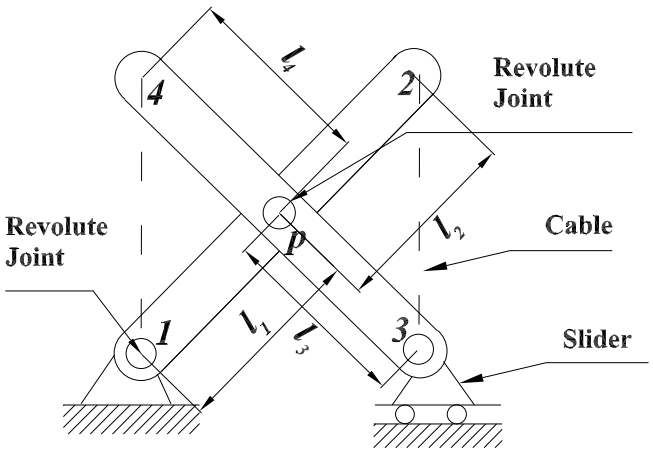

Figure 1: Basic planar module of SLE

of the SLEs. The cables are taut in the fully deployed configuration and slack at all other configurations. One active cable which is firmly connected to the joint 3 of SLE mast, runs over a pulley at joint 4, zig-zags down the SLE following the route shown in the figure (it runs over a pulley at each kink) and, after passing over a pulley at joint 1, is connected to the motorised drum located below the base. This mast remains stress free during folding. It can be deployed simply by turning the drum below the base and thus winding in the active cable. When the passive cable is taut the deployment is complete. At this stage the active cable is wound in little more to set up a state of self stress in the system. Usually it is desirable that all the passive cables be in a state of pretension while the structure is operational to avoid the possibility of some of them might going slack when the mast is subjected to the action of external loads; it is easiest to aim for uniform state of prestress in all cables. The uniform pre-stress can be obtained by introducing the second active cable [3].

The triangular SLE mast can be created with three SLE's. The stacked triangular SLE mast [2] is shown in figure 3. This has twelve passive cables and an active cable. The active cable is firmly attached to joint 5. The double loops are connected at the intermediate joints

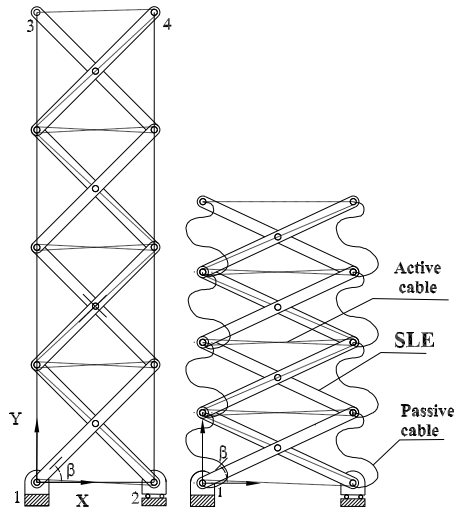

Figure 2: Stacked planar SLE mast – (a) Fully deployed and (b) Partially deployed

as shown in figure 3. This pre-tensions uniformly all the cables in the mast. A drum is used to wind the active cable.

The function of passive cables are a) for termination of deployment, b) increasing the stiffness of fully deployed structure, and c) setup a state of pre-stress in the fully deployed structure resulting in pre-tensioning of all passive cables. An active cable is such that its length reduces monotonically as the structure deploys. The functions of active cable is to a) control the deployment process, b) setup a state of pre-stress in a fully deployed structure resulting in pre-tensioning the whole system, and c) elimination of backlash at all joints. More than one active cable is often introduced in some structure. In practice it is advisable to have no less than two active cables to ensure minimum level of redundancy should an active cable fail. However it is impractical to introduce many active cables in the structure because different cables may require independent winding mechanisms and control units. A structure with passive and active cables remains essentially stress free in folded/partially folded configurations and is pre-stressed in the fully deployed state. These structures have

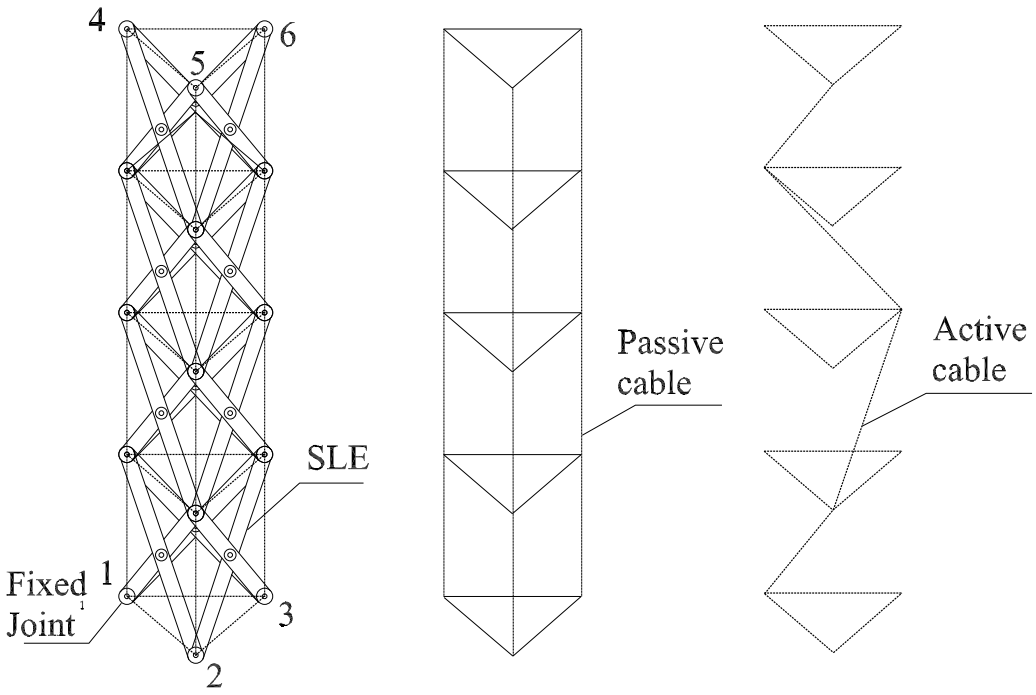

Figure 3: Stacked triangular SLE mast – (a) Full mast, (b) Passive cables, and (c) Active cable

high stiffness when fully deployed.

2.1 Formulation of constraints

In this section we derive the kinematic constraint equations for the SLE. We will use the Cartesian/natural coordinates [6] to model the SLE. The natural or Cartesian coordinates are defined at the locations of the joints and unit vectors along the joint axis to define the motion of the link completely. In the natural coordinate system the constraint equations originate in the form of rigid constraints of links and joint constraints.

Consider a SLE shown in figure 1. This is considered as an assembly of two links $1-2$ and $3-4$ with a pivot p. The link $1-2$ with pivot p is considered as an assembly of two

link segments $1-p$ and $p-2$ with lengths l_1 and l_2, respectively. Likewise, the link $3-4$ with pivot p is considered as an assembly of two link segments $3-p$ and $p-4$ with lengths l_3 and l_4, respectively.

2.1.1 Rigid link constraint

A rigid link is characterized by a constant distance between two natural coordinates i and j. This is given by

$$\mathbf{r}_{ij} \cdot \mathbf{r}_{ij} = L_{ij}^2 \tag{3}$$

where $\mathbf{r}_{ij} = [(X_i - X_j), (Y_i - Y_j), (Z_i - Z_j)]^T$ with (X_i, Y_i, Z_i), (X_j, Y_j, Z_j) are the natural coordinates of i, j, respectively, and L_{ij} is the distance between i and j.

Using this equation for the SLE of figure 1 we get the following systems of equations for the four segments:

$$\begin{aligned}
(X_p - X_1)^2 + (Y_p - Y_1)^2 + (Z_p - Z_1)^2 - l_1^2 &= 0 \\
(X_2 - X_p)^2 + (Y_2 - Y_p)^2 + (Z_2 - Z_p)^2 - l_2^2 &= 0 \\
(X_3 - X_p)^2 + (Y_3 - Y_p)^2 + (Z_3 - Z_p)^2 - l_3^2 &= 0 \\
(X_p - X_4)^2 + (Y_p - Y_4)^2 + (Z_p - Z_4)^2 - l_4^2 &= 0
\end{aligned} \tag{4}$$

2.1.2 Constraint for SLE

Referring to figure 1, the node p is a pivot, the link segments $1-p$ and $p-2$ of link $1-2$ are aligned at pivot. Hence, the cross product of the two adjacent link segments $1-p$ and $p-2$ is given by

$$\mathbf{r}_{1p} \times \mathbf{r}_{p2} - l_1 l_2 \sin\phi_1 = 0 \tag{5}$$

where, ϕ_1 is the angle between the two link segments (equal to 0 degrees for a pantograph mast). Similarly the constraint equation for the link 34 is given by

$$\mathbf{r}_{3p} \times \mathbf{r}_{p4} - l_3 l_4 \sin\phi_2 = 0 \tag{6}$$

where, ϕ_2 the angle between the two link segments (0 degree in our case). The equations (5), (6) along with rigid link constraint equations (equation (4)) of the four link segments $1p$, $p2$, $3p$ and $p4$ form the complete set of equations for a single SLE.

2.1.3 System constraint equations

The rigid constraint equations and joint constraints of SLE can be written together as

$$f_j(X_1, Y_1, Z_1, X_2, \cdots, Z_n) = 0 \quad \text{for } j = 1, \ldots, n_c \tag{7}$$

where, n_c represents the total number of constraint equations including rigid link and joint constraints of SLE, and $n_t = 3n$ is the total number of Cartesian coordinates of the system. The derivative of the constraint equations give the Jacobian matrix and can be symbolically written as

$$[\mathbf{J}]\delta\mathbf{X} = \mathbf{0} \tag{8}$$

Since, equation (8) is homogeneous, one can obtain a non-null $\delta\mathbf{X}$ if the dimension of the null-space of $[\mathbf{J}]_{n_c \times n_t}$ is at least one. The existence of the null-space implies that the mechanism possess a degree of freedom along the corresponding $\delta\mathbf{X}$ [6]. The null space of $[\mathbf{J}]$ can be obtained numerically.

The dimension of the null space is the degree of freedom/mobility of the deployable system. The deployable systems will have large number of links and joints arranged in a repetitive pattern. Using the above equations one can evaluate the possible change in degree of freedom of the deployable system with addition of each link/joints and also can identify the redundant links/joints in the system [9].

The deployable systems at the end of deployment lock and the cables attached to the successive joints get prestressed there by reducing the mechanism to a structure. Using the null space dimension of the Jacobian matrix one can evaluate the minimum number of cables required to reduce the mechanism to structure.

3 Stiffness matrix for the SLE

In this section we present a method to evaluate the stiffness matrix for SLE from the constraint Jacobian matrix discussed in the previous section. The SLE is considered to have constant cross sectional area and uniform material properties. The cross section of the SLE remains plane and perpendicular to the longitudinal axis during deformation. The longitudinal axis which lies within the neutral surface does not experience any change in length. The SLE beam is long and slender and the transverse shear and rotary inertia effects are negligible. These assumptions allows the use of Euler-Bernoulli beam theory.

3.1 Stiffness matrix from length constraints

From the length constraint equations, the elongation in the structural members, $\delta\mathbf{L}$, can be related to the system displacements, $\delta\mathbf{X}$, as

$$[\mathbf{J}_m]\delta\mathbf{X} = \delta\mathbf{L} \tag{9}$$

where the Jacobian matrix, $[\mathbf{J}_m]$, can be obtained from equations (4) (see Appendix) and $\delta\mathbf{X}$, $\delta\mathbf{L}$ are given by

$$\begin{aligned} \delta\mathbf{X} &= [\delta X_1, \delta Y_1, \delta Z_1, \delta X_2, \delta Y_2, \delta Z_2, \delta X_3, \delta Y_3, \delta Z_3, \delta X_4, \delta Y_4, \delta Z_4, \delta X_p, \delta Y_p, \delta Z_p]^T \\ \delta\mathbf{L} &= [\delta l_1, \delta l_2, \delta l_3, \delta l_4]^T \end{aligned}$$

If the elongation $\delta\mathbf{L}$ are elastic, the member forces, $\delta\mathbf{T}$, can be expressed with a diagonal matrix of member stiffnesses as given below.

$$[\mathbf{S}_m]\delta\mathbf{L} = \delta\mathbf{T} \tag{10}$$

where, the member stiffness matrix $[\mathbf{S}_m]$ for the length segments of SLE is given by

$$[\mathbf{S}_m] = \begin{bmatrix} \frac{A_1 E_1}{l_1} & 0 & 0 & 0 \\ 0 & \frac{A_2 E_2}{l_2} & 0 & 0 \\ 0 & 0 & \frac{A_3 E_3}{l_3} & 0 \\ 0 & 0 & 0 & \frac{A_4 E_4}{l_4} \end{bmatrix}$$

In the above equation E is the Young's modulus, A the cross sectional area the diagonal elements correspond to the axial stiffness due to elongation of the link segments, and $\delta\mathbf{T} = [\delta T_1, \delta T_2, \delta T_3, \delta T_4]^T$ are the forces in the link segments.

The equilibrium matrix for the reference configuration can be written in terms of the transpose of the Jacobian matrix and we can write

$$[\mathbf{J}_m]^T \delta\mathbf{T} = \delta\mathbf{F} \tag{11}$$

where $\delta\mathbf{F}$ is given by

$$\delta\mathbf{F} = [\delta F_{1x}, \delta F_{1y}, \delta F_{1z}, \delta F_{2x}, \delta F_{2y}, \delta F_{2z}, \delta F_{3x}, \delta F_{3y}, \delta F_{3z}, \delta F_{4x}, \delta F_{4y}, \delta F_{4z}, \delta F_{px}, \delta F_{py}, \delta F_{pz}]^T$$

with the right-hand side denoting the load components at nodes.

To be statically determinate, the load must be in the column space of the equilibrium matrix, in which case it is the equilibrium load. Substituting the equations (9) and (10) in equation (11), we get

$$[\mathbf{J}_m]^T [\mathbf{S}_m][\mathbf{J}_m]\delta\mathbf{X} = \delta\mathbf{F} \tag{12}$$

The above equation can be written as

$$[\mathbf{K}_m]\delta\mathbf{X} = \delta\mathbf{F} \tag{13}$$

where, $[\mathbf{K}_m] = [\mathbf{J}_m]^T[\mathbf{S}_m][\mathbf{J}_m]$ is the elastic stiffness matrix of four length segments of the SLE.

3.2 Stiffness matrix due to bending

The rotations $\delta\phi$ in the structural members can be obtained from the cross-product equations (5)-(6) of SLE. The rotations are the constraint variations related to the system displacements $\delta\mathbf{X}$ and in terms of the Jacobian matrix $[\mathbf{J}]$ are given as

$$\begin{aligned} [\mathbf{J}_{12}]\,\delta\mathbf{X}_{12} &= \delta\phi_1 \\ [\mathbf{J}_{34}]\,\delta\mathbf{X}_{34} &= \delta\phi_2 \end{aligned} \tag{14}$$

The detailed matrix is given in Appendix.

In the above equation $\delta\mathbf{X}_{12}$ is the vector $[\delta X_1, \delta Y_1, \delta Z_1, \delta X_2, \delta Y_2, \delta Z_2, \delta X_p, \delta Y_p, \delta Z_p]^T$ and $\delta\mathbf{X}_{34}$ is the vector $[\delta X_3, \delta Y_3, \delta Z_3, \delta X_4, \delta Y_4, \delta Z_4, \delta X_p, \delta Y_p, \delta Z_p]^T$. These are the displacements of the link $1-p-2$ and $3-p-4$, respectively. Finally, $\delta\phi_\mathbf{1} = [\delta\phi_{1x}, \delta\phi_{1y}, \delta\phi_{1z}]^T$ and $\delta\phi_\mathbf{2} = [\delta\phi_{2x}, \delta\phi_{2y}, \delta\phi_{2z}]^T$ are the rotations in the global coordinate system.

The transformation matrix relating the global and local coordinate system is given by

$$\begin{aligned} \delta\phi_1' &= [\mathbf{R}]\,\delta\phi_1 \\ \delta\phi_2' &= [\mathbf{R}]\,\delta\phi_2 \end{aligned} \tag{15}$$

where $\delta\phi_1'$ and $\delta\phi_2'$ are the rotations in the local coordinate system and $[\mathbf{R}]$ is the transformation matrix relating the local and global coordinate systems [22]. The transformation matrix $[\mathbf{R}]$ is given by

$$[\mathbf{R}] = [\mathbf{R}_\Theta][\mathbf{R}_\Phi][\mathbf{R}_\Psi] \tag{16}$$

where,

$$[\mathbf{R}_\Psi] = \begin{bmatrix} \frac{C_x}{\sqrt{{C_x}^2+{C_z}^2}} & 0 & \frac{C_z}{\sqrt{{C_x}^2+{C_z}^2}} \\ 0 & 1 & 0 \\ \frac{-C_z}{\sqrt{{C_x}^2+{C_z}^2}} & 0 & \frac{C_x}{\sqrt{{C_x}^2+{C_z}^2}} \end{bmatrix}$$

$$[\mathbf{R}_\Phi] = \begin{bmatrix} \sqrt{{C_x}^2 + {C_z}^2} & C_y & 0 \\ -C_y & \sqrt{{C_x}^2 + {C_z}^2} & 0 \\ 0 & 0 & 1 \end{bmatrix}$$

$$[\mathbf{R}_\Theta] = \begin{bmatrix} 1 & 0 & 0 \\ 0 & \cos\Theta & \sin\Theta \\ 0 & \sin\Theta & \cos\Theta \end{bmatrix}$$

where, for the nodes i and j with length L, $C_x = \frac{X_i - X_j}{L}$,$C_y = \frac{Y_i - Y_j}{L}$, $C_z = \frac{Z_i - Z_j}{L}$ and Θ is the angle from one of the principal axis of cross section of SLE beam. Using equations (14) and (15) we get

$$\begin{aligned} \delta\phi_1' &= [\mathbf{R}][\mathbf{J}_{12}]\delta\mathbf{X}_{12} \\ \delta\phi_2' &= [\mathbf{R}][\mathbf{J}_{34}]\delta\mathbf{X}_{34} \end{aligned} \tag{17}$$

Considering the bending deformation of the links and neglecting torsion the above equations can be written as

$$\begin{aligned} \delta\phi_1'' &= [\mathbf{J}_1]\delta\mathbf{X}_{12} \\ \delta\phi_2'' &= [\mathbf{J}_2]\delta\mathbf{X}_{34} \end{aligned} \tag{18}$$

where, $\delta\phi_{\mathbf{1}}{}'' = [\delta\phi_{1y}', \delta\phi_{1z}']^T$ and $\delta\phi_{\mathbf{2}}{}'' = [\delta\phi_{2y}', \delta\phi_{2z}']^T$.

Combining the above equations, we can write

$$\delta\phi'' = [\mathbf{J}_n]\delta\mathbf{X} \tag{19}$$

where, $\delta\phi'' = [\delta\phi_{\mathbf{1}}{}'', \delta\phi_{\mathbf{2}}{}'']^T$. The relation between the forces and moments is given by

$$\delta\mathbf{F} = [\mathbf{J}_n^T]\delta\mathbf{M}'' \tag{20}$$

where, $\delta\mathbf{M}'' = [\delta M_{12y}', \delta M_{12z}', \delta M_{34y}', \delta M_{34z}']^T$.

If the rotations $\delta\phi''$ are elastic, the member moments $\delta\mathbf{M}''$ can be expressed with a diagonal matrix of member stiffnesses as given below.

$$[\mathbf{S}_n]\delta\phi'' = \delta\mathbf{M}'' \tag{21}$$

where, the member stiffness matrix $[\mathbf{S}_n]$ for the SLE is given by

$$[\mathbf{S}_n] = \begin{bmatrix} \frac{3E_1I_z}{l_1+l_2} & 0 & 0 & 0 \\ 0 & \frac{3E_1I_y}{l_1+l_2} & 0 & 0 \\ 0 & 0 & \frac{3E_2I_z}{l_3+l_4} & 0 \\ 0 & 0 & 0 & \frac{3E_2I_y}{l_3+l_4} \end{bmatrix}$$

In the above equation E is the Young's modulus, I_z and I_y are the second moment of area of cross section about Z and Y axes, respectively, and the diagonal elements correspond to the bending stiffness of the links $1-p-2$ and $3-p-4$ about Z and Y axis.

By using a similar procedure as given in previous section, the final equations can be obtained by substituting the equations (19), (21) in (20). We get

$$[\mathbf{J}_n]^T[\mathbf{S}_n][\mathbf{J}_n]\delta\mathbf{X} = \delta\mathbf{F} \tag{22}$$

and this equation can be written as

$$[\mathbf{K}_n]\delta\mathbf{X} = \delta\mathbf{F} \tag{23}$$

where, $[\mathbf{K}_n] = [\mathbf{J}_n]^T[\mathbf{S}_n][\mathbf{J}_n]$ is the elastic stiffness matrix for the SLE. By combining the stiffness matrix due to length constraint equations (13) and SLE constraint equations (23), we get

$$[\mathbf{K}_s]\delta\mathbf{X} = \delta\mathbf{F} \tag{24}$$

where, $[\mathbf{K}_s] = [\mathbf{K}_m] + [\mathbf{K}_n]$ is the elastic stiffness matrix due to length and SLE constraints

3.3 Rank of stiffness matrix

The stiffness matrix is given by

$$[\mathbf{K}_s] = [\mathbf{J}_s]^T[\mathbf{S}_s][\mathbf{J}_s] = [\mathbf{J}_s]^T([\mathbf{S}_s^*]^T[\mathbf{S}_s{}^*])[\mathbf{J}_s] = ([\mathbf{J}_s][\mathbf{S}_s^*)]^T([\mathbf{J}_s][\mathbf{S}_s^*]) \tag{25}$$

where $[\mathbf{S}_s{}^*]$ is a diagonal matrix whose elements are square root of $[\mathbf{S}_s]$, $[\mathbf{J}_s]$ is the Jacobian matrix of the single SLE. Since for a regular bar frame works all elements from $[\mathbf{S}_s]$ are

positive, the rank of $[\mathbf{J}_s][\mathbf{S}_s^*]$ takes it value from the rank of $[\mathbf{J}_s]$. Furthermore

$$rank([\mathbf{K}_s]) = rank(([\mathbf{J}_s][\mathbf{S}_s])^T([\mathbf{J}_s][\mathbf{S}_s])) = rank([\mathbf{J}_s][\mathbf{S}_s]) = rank([\mathbf{J}_s]) \tag{26}$$

3.4 Comparison with other methods

In reference [15], the displacement method was used to derive the stiffness matrix. The link $1-2$ is also called as an uniplet in the reference paper. By using the first two length constraint equations in (4) of the link $1-p-2$ and the SLE constraint equation (5) we can formulate the Jacobian matrix. The stiffness matrix for the uniplet can be computed by using equation (24). It can be observed that the stiffness matrix, obtained by our method, matches exactly with the matrix formulated in reference [15] by the displacement method.

In reference [14], the authors have used force method to arrive at the stiffness matrix. Using the length constraint equations (4) and SLE constraint equations (5), (6) we can formulate the Jacobian matrix as described in the previous section. By using the coordinate system of reference [14] and making the substitutions in Jacobian matrix equation (8), we can observe that matrix obtained by our method is same as the matrix shown in equation(37) of reference [14] obtained by the force method. It can be observed that the transpose of this matrix relates the forces and the moments of SLE.

4 Equation for the cable

As already described earlier, cables are added in the masts to enhance their stiffness. These cables are slack in the stowed configuration and are taut at the end of deployment. A cable can be assumed to be bar in the taut configuration. The stiffness matrix for the bar may be found in many textbooks and is described below for completeness. For the bar shown in figure 4 connecting the joints i and j, the stiffness matrix is given by

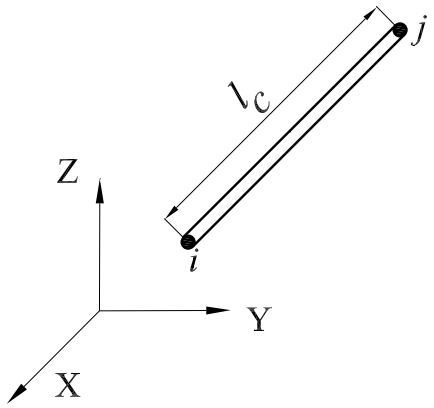

Figure 4: Typical truss element with coordinates

$$[\mathbf{K}_c] = \frac{A_c E_c}{l_c} \begin{bmatrix} r^2 & rs & rt & -r^2 & -rs & -rt \\ rs & s^2 & st & -rs & -s^2 & -st \\ rt & st & t^2 & -rt & -st & -t^2 \\ -r^2 & -rs & -rt & r^2 & rs & rt \\ -rs & -s^2 & -st & rs & s^2 & st \\ -rt & -st & -t^2 & rt & st & t^2 \end{bmatrix}$$

where, $r = \frac{X_i - X_j}{l_c}$, $s = \frac{Y_i - Y_j}{l_c}$ and $t = \frac{Z_i - Z_j}{l_c}$. In the above equation cross sectional area is denoted by A_c, Young's modulus is denoted by E_c and the bar/cable length is denoted by l_c.

By combining the stiffness matrix of SLE elements and the cable we can write

$$[\mathbf{K}]\delta\mathbf{X} = \delta\mathbf{F} \tag{27}$$

where the total stiffness matrix $[\mathbf{K}]$ is given by $[\mathbf{K}_s] + [\mathbf{K}_c]$.

5 Revolute joint constraints

The two adjacent SLE's are connected by revolute joints as shown in figure 5. This enforces additional constraints of the form

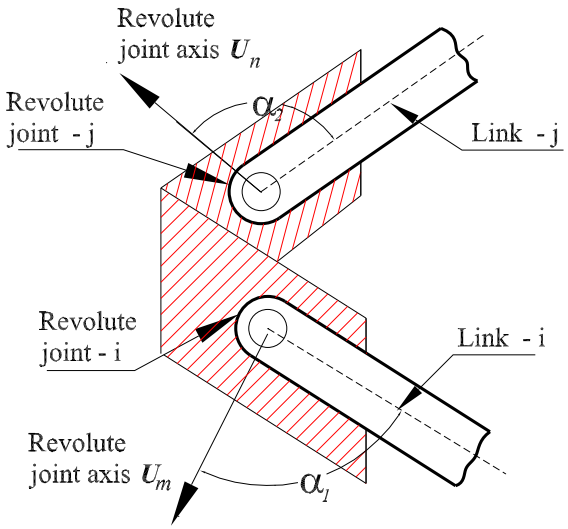

Figure 5: A spherical joint replaced by two revolute joints

$$\begin{aligned} \mathbf{r}_{ip} \cdot \mathbf{U}_m - L_{ip}\cos(\alpha_1) &= 0 \\ \mathbf{r}_{jq} \cdot \mathbf{U}_n - L_{jq}\cos(\alpha_2) &= 0 \end{aligned} \tag{28}$$

where the unit vectors $\mathbf{U}_m$ and $\mathbf{U}_n$ are along the revolute joint axis as shown in figure 5. The angles α_1 and α_2 are the angles between the unit vectors and $\mathbf{r}$. In our approach, Lagrange multiplier is used to enforce these constraints on the stiffness matrix equations presented in the previous section.

5.1 Lagrange multiplier method

For a steady state discrete linear system with potential energy functional Π^* expressed by

$$\Pi^* = \frac{1}{2}\mathbf{U}^T[\mathbf{K}]\mathbf{U} - \mathbf{U}^T\mathbf{F} \tag{29}$$

where, $\mathbf{U}$ is the displacement of the structural system, $[\mathbf{K}]$ is the stiffness matrix and $\mathbf{F}$ is the external load, the equilibrium equations can be found for the condition which make the variation of Π^* stationary. We get

$$\delta\Pi^* = \delta\mathbf{U}^T([\mathbf{K}]\mathbf{U} - \mathbf{F}) = 0 \tag{30}$$

with respect to the admissible virtual displacements $\delta\mathbf{U}$. Since $\delta\mathbf{U}$ is arbitrary the above equation yields

$$[\mathbf{K}]\mathbf{U} = \mathbf{F} \tag{31}$$

The constraint equations due to revolute joints can be written in the general form as

$$\phi(\mathbf{U}) = [\mathbf{C}]\mathbf{U} - \mathbf{D} = \mathbf{0} \tag{32}$$

where $[\mathbf{C}]_{p\times q}$ is the constraint matrix, p is the number of constraint equations, q is the number of variables and $\mathbf{D}$ is a vector of constants.

In the Lagrange multipliers method the potential function is appended with the revolute joint constraints and we get

$$\Pi = \Pi^* + \lambda^T\phi(\mathbf{U}) \tag{33}$$

where, $\lambda = [\lambda_1, \ldots, \lambda_p]$ are the Lagrange multipliers. The stationary of this functional Π is

$$\delta\Pi = \delta\Pi^* + \delta\mathbf{U}^T(\mathbf{C}^T\lambda) + \delta\lambda^T(\mathbf{C}\mathbf{U} - \mathbf{D}) = 0 \tag{34}$$

For arbitrary $\delta\lambda$ and $\delta\mathbf{U}$ the above equation gives

$$\begin{bmatrix} K & C^T \\ C & 0 \end{bmatrix} \begin{Bmatrix} \mathbf{U} \\ \lambda \end{Bmatrix} = \begin{Bmatrix} \mathbf{F} \\ \mathbf{D} \end{Bmatrix} \tag{35}$$

The advantage of Lagrange multiplier method is that the constraints are satisfied exactly but this is at the expense of larger set of equations. This method also gives the magnitudes of constraint forces since the Lagrange multipliers can be obtained by solving equation (35).

6 Results and discussions

In this section, the degree of freedom and the redundancy of the joints/links are first obtained for a hexagonal mast. The stiffness of the mast is then evaluated and the variation in stiffness with addition of cables is presented. We also present the stiffness evaluation for an assembly of four hexagonal masts.

6.1 Degree of freedom and redundancy evaluation

The hexagonal mast built out of SLE's,is presented in figure 6. The mast has six SLEs. Each SLE has 4 rigid link constraints and 6 SLE constraint equations at the pivot point. Fixed boundary conditions are used at joint 1. The coordinates of joints of the mast are presented in Table 1. The results of null space analysis of the constraint Jacobian matrix are presented in Table 2. It is observed from the table that the dimension of null space reduces on adding each SLE and the null space does not change for the last SLE. Hence, the last SLE is redundant. The above analysis assumes spherical joints for the points connected by the adjacent SLEs. The revolute joint constraints are added further for each face and null space is evaluated. It can be observed from the table that the null space reduces for addition of revolute joints on each face. The null space does not change for the revolute joints added for the face 5 and face 6. Hence these joints are redundant.

By adding the boundary condition the mast will be a single degree of freedom system. It can be observed that the last SLE and the revolute joints on the face 5 and face 6 are redundant from the kinematic point of view. In order to reduce this mast to a structure a cable can be added at any two successive joints. The simulation is further continued by adding a cable between the joint 1 and joint 2. The null space dimension of the Jacobian matrix is zero indicating that the mast a structure.

Joints	X Coordinate(mm)	Y Coordinate(mm)	Z Coordinate(mm)
Joint 1	0.0	0.0	0.0
Joint 2	500.0	-866.0254	0.0
Joint 3	1500.0	-866.0254	0.0
Joint 4	2000.0	0.0	0.0
Joint 5	1500.0	866.0254	0.0
Joint 6	500.0	866.0254	0.0
Joint 7	0.0	0.0	700.0
Joint 8	500.0	-866.0254	700.0
Joint 9	1500.0	-866.0254	700.0
Joint 10	2000.0	0.0	700.0
Joint 11	1500.0	866.0254	700.0
Joint 12	500.0	866.0254	700.0

Table 1: Input data: coordinates of joints for hexagonal mast

Contents	Size of [**J**]	Null Space	Remarks
+ SLE 1	(20,39)	21	
+ SLE 2	(28,42)	18	
+ SLE 3	(36,45)	15	
+ SLE 4	(44,48)	12	
+ SLE 5	(52,51)	10	
+ SLE 6	(60,54)	10	SLE - 6 is redundant
+ FACE 1	(62,54)	8	
+ FACE 2	(64,54)	6	
+ FACE 3	(66,54)	5	
+ FACE 4	(68,54)	4	
+ FACE 5	(70,54)	4	Revolute joints are redundant
+ FACE 6	(72,54)	4	Revolute joints are redundant
+ Boundary conditions ($X_1 = Y_1 = Z_1 = 0$)	(75,54)	1	Mechanism
+ Cable 1-2	(76,54)	0	Structure

Table 2: [**J**] matrix details for hexagonal mast

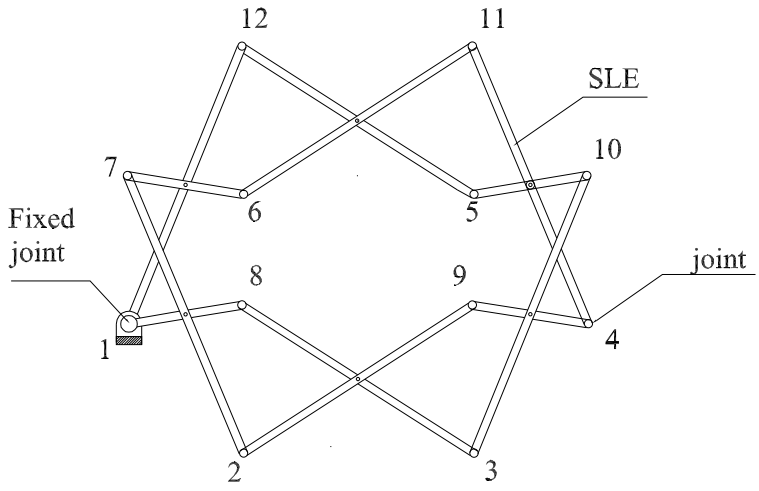

Figure 6: Hexagonal SLE mast in the deployed configuration

6.2 Stiffness evaluation

In this section the stiffness matrix(see equation (24)) developed in previous section for the SLE is used along with the Lagrange multiplier (see equation (35)) to evaluate the stiffness of the mast.

Figure 7 shows the two-dimensional straight deployable structure consisting of four pantograph units presented in reference [14] and an active cable zig-zagging across the pantograph. A constant tension spring keeps the active cable pre-tensioned in all configurations. The structure is deployed from nearly flat $\beta = 1.0$ degree to the configuration shown in figure 7, $\beta = 45$ degrees, by shortening gradually the active cable. The cables have $AE = 1.5 \times 10^5$ N and the pantograph units have $AE = 3.5 \times 10^6$ N and $EI_z = 9.6 \times 10^7 \text{Nmm}^2$. The length of arm is 1000 mm. The tip stiffness of the assembly as it deploys is evaluated by applying two forces of 0.5 N to top joints in X and Y directions. Figure 8 presents the axial and lateral stiffness of the system. These results matches with those presented in literature [14].

Figure 9 shows a hexagonal mast in the deployed configuration. This mast has six SLEs and the six cables in the top, six cables in the bottom and six vertical cables are connected

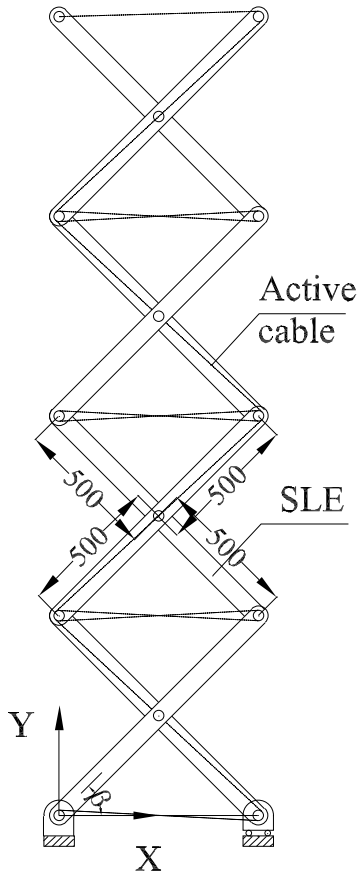

Figure 7: Stacked SLE units of reference [14]

as shown in the figure. These cables are slack during deployment and becomes taut at the end of deployment. The SLE and cables have the cross sectional area, A, of $138.23mm^2$ and $1.0mm^2$ respectively. the Young's Modulus E of the SLE and cables are 70000.0 N/mm^2 and 63000.0 N/mm^2 respectively. The second moment of inertia I_z, of SLE is 8432.0 mm^4. An unit load is applied at joint 10. The stiffness of the mast due to these loads were found to be 31.73N/mm, 138.72N/mm and 23.85N/mm in X, Y and Z direction respectively.

In order to study the sensitivity of the mast stiffness with cables the simulations were

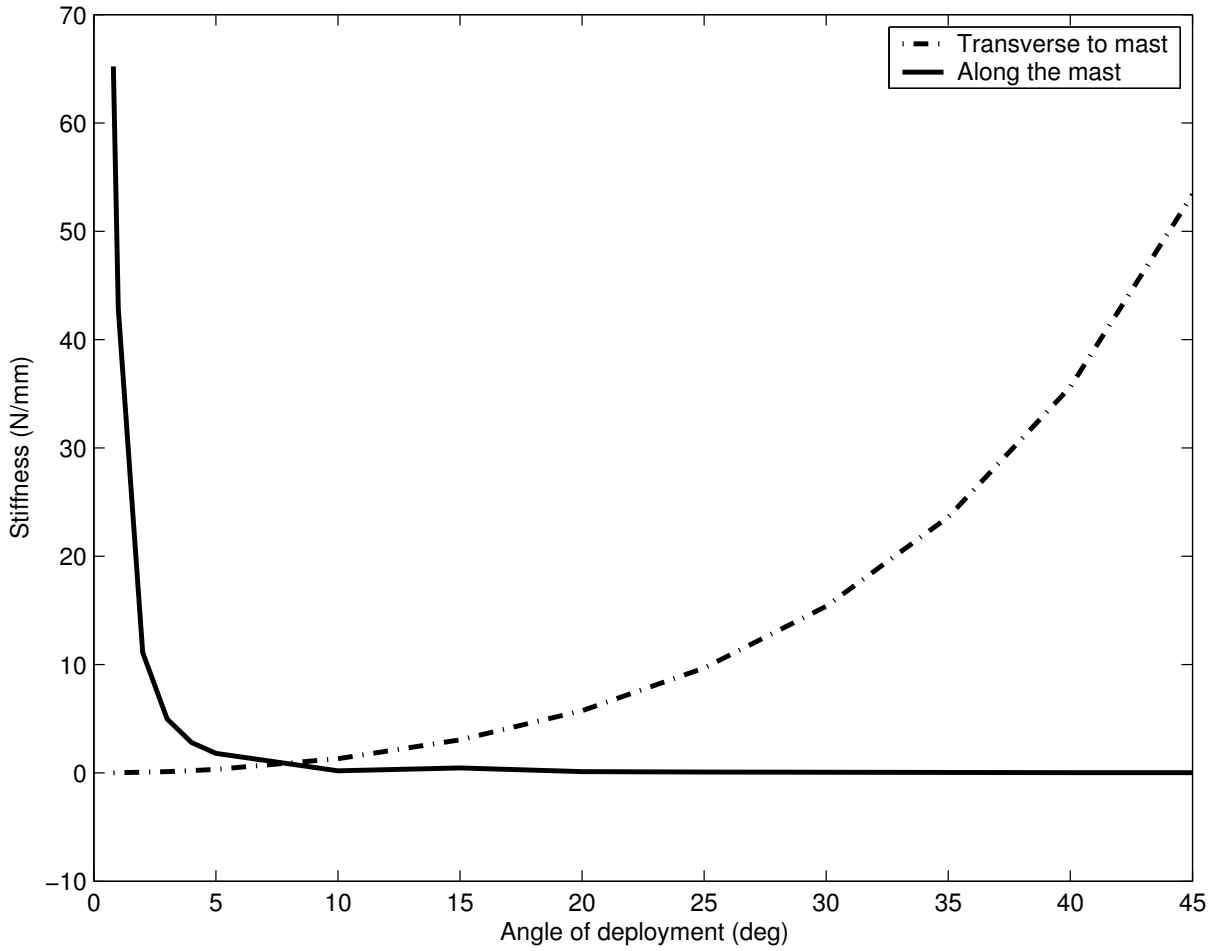

Figure 8: Axial and lateral stiffness during deployment

carried out by adding top, bottom and vertical cables individually and in combinations. The results are presented in Table 3. It can be observed that the stiffness does not increase significantly when either top, bottom or vertical cables are used individually. The stiffness increases by more than 50% when top and bottom cables are used together. The stiffness further increases by additional 30% or more when all three cables, namely top, bottom and vertical, are used together. The stiffness in Y direction is found to be higher than in the other two directions.

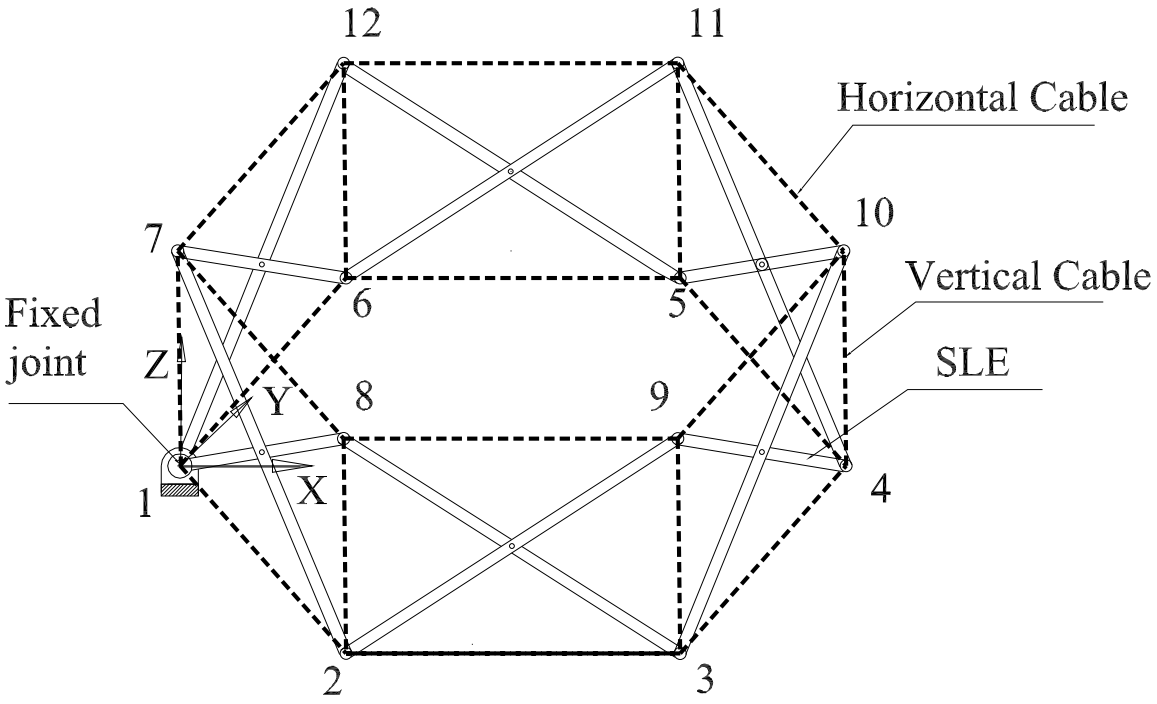

Figure 9: Hexagonal SLE mast in the deployed configuration with cables

Figure 10 shows a deployed mast consisting of four hexagonal masts. This mast has nineteen SLEs and the nineteen cables in the top, nineteen cables in the bottom and sixteen vertical cables are connected as shown in the figure. Fixed boundary conditions are used at joint 1. The coordinates of the bottom joints of the mast are presented in Table 4. The other coordinates are symmetrical. The top coordinates are located at 700 mm along Z axis. The cables are slack during deployment and becomes taut at the end of deployment. The geometrical and material properties of the SLE and cables are same as in the example of the single hexagonal mast presented earlier. An unit load is applied at joint 31. The stiffness of the mast due to these loads were found to be 114.23N/mm, 326.64N/mm and 39.26N/mm in X, Y and Z direction respectively.

In order to study the sensitivity of the mast stiffness with cables the simulations were

	Stiffness in X direction (N/mm)	Stiffness in Y direction (N/mm)	Stiffness in Z direction (N/mm)
Mast with top or bottom cables	24.27	53.24	11.32
Mast with only vertical cables	27.88	30.48	7.39
Mast with top and bottom cables	28.61	98.36	18.33
Mast with all cables	31.73	138.72	23.85

Table 3: Variation of stiffness with addition of cables for hexagonal mast

Joints	X Coordinate(mm)	Y Coordinate(mm)	Z Coordinate(mm)
Joint 1	0.0	0.0	0.0
Joint 2	500.0	-866.0254	0.0
Joint 3	1500.0	-866.0254	0.0
Joint 4	2000.0	0.0	0.0
Joint 13	2000.0	-1732.10	0.0
Joint 14	3000.0	-1732.10	0.0
Joint 15	3500.0	-866.0254	0.0
Joint 16	3000.0	0.0	0.0
Joint 27	4500.0	-866.0254	0.0
Joint 28	5000.0	0.0	0.0

Table 4: Input data: coordinates of joints for assembled hexagonal mast

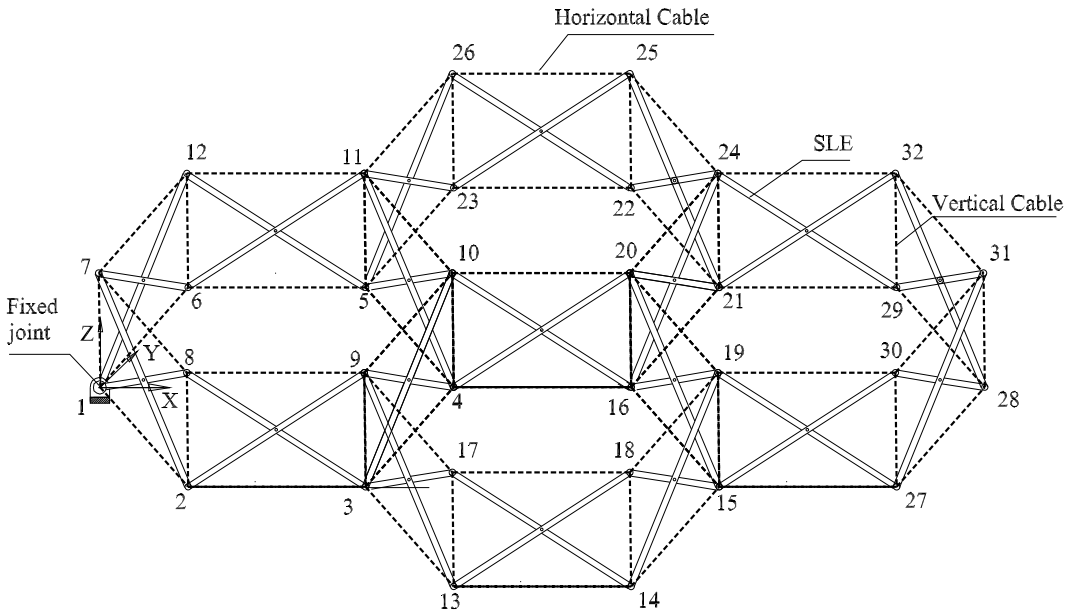

Figure 10: Assembly of four hexagonal masts in the deployed configuration with cables

carried out by adding top, bottom and vertical cables individually and in combinations. The results are presented in Table 5. It can be observed that the stiffness does not increase significantly when either top, bottom or vertical cables are used individually. The stiffness increases by more than 55% when top and bottom cables are used together. The stiffness further increases by additional 45% or more when all three cables, namely top, bottom and vertical, are used together. The stiffness in Y direction is found to be higher than in the other two directions.

7 Conclusions

In this paper, Cartesian coordinates and symbolic computations have been used for kinematic and static analysis of three dimensional deployable SLE masts. The mobility of the masts

	Stiffness in X direction (N/mm)	Stiffness in Y direction (N/mm)	Stiffness in Z direction (N/mm)
Mast with top or bottom cables	32.01	104.31	17.56
Mast with only vertical cables	40.46	81.17	10.28
Mast with top and bottom cables	65.44	175.42	27.25
Mast with all cables	114.23	326.64	39.26

Table 5: Variation of stiffness with addition of cables for assembled hexagonal mast

were evaluated from the dimension of null space of the Jacobian matrix formed by the derivative of the constraint equations. The stiffness matrix for the SLE was obtained from the constraint Jacobian. The stiffness matrix obtained by our approach is same as those obtained with the force and displacement methods of literature. The main advantage of the constraint Jacobian based approach are a) ease of obtaining the stiffness matrices, b) determination of mobility and the redundant joints/links of the mast, and c) ease of incorporating revolute joint constraints by using Lagrange multipliers. The stiffness due to cables, an integral part of deployable masts, are also considered. The constraint Jacobian approach was used for the analysis of a hexagonal mast and a assembled hexagonal mast, and the stiffness of the masts in different directions were obtained. The approach presented in this paper can be extended to masts of different shapes and to stacked masts.

References

[1] A K S Kwan, S Pellegrino. A cable rigidized 3D pantograph, *Proc. of 4rth European symposium on Mechanisms and Tribology*, France, Sept. 1989 (ESA-S P-299, March 1990).

[2] Z You, S Pellegrino. Cable stiffened pantographic deployable structures, Part1: Triangular mast. AIAA Journal 1996;34(4):813-20.

[3] A K S Kwan, S Pellegrino. Active and passive elements in deployable/retractable masts. International Journal of Space Structures 1993;8(1-2):29-40

[4] R S Hartenberg, J Denavit. *Kinematic Synthesis of Linkages*, McGraw Hill, 1965.

[5] *MSC Adams Users Manual*, MSC Software Corporation, USA.

[6] J Garcia De Jalon, E Bayo. *Kinematic and dynamic simulation of multi-body systems: The real time challenge*. Springer Verlag, 1994.

[7] J. Garcia De Jalon, Migual Angel Serna. Computer methods for kinematic analysis of lower pair mechanism -1 Velocities and acceleration. Mechanism and Machine Theory 1982;17(6):397-03.

[8] J Garcia De Jalon, J Unda and A. Avello. Natural coordinates of computer analysis of multi body systems. Computer Methods in Applied Mechanics and Engineering 1986;56:309-27.

[9] B P Nagaraj, R Pandiyan and A Ghosal. Kinematics of pantograph masts. Mechanism and Machine Theory 2009;44(4):822-34

[10] C R Calladine. Buckminister Fuller's "Tensigrity" structure and Clerk Maxwell's rule for the construction of stiff frames. International Journal of Solids and Structures 1978; 14:161-72.

[11] F Freudenstein. On the verity of motions generated by mechanism. Journal of Engineering for Industry, Transactions of ASME 1962;84:156-60.

[12] E N Kuznetsov. Under constrained structural systems. International Journal of Solids and Structures 1988; 24(2):153-63.

[13] E N Kuznetsov. Orthogonal load resolution and statical-kinematic stiffness matrix. International Journal of Solids and Structures 1997;34(28):3657-72.

[14] A K S Kwan, S Pellegrino. Matrix formulation of macro-elements for deployable structures. Computers and Structures 1994;50(2):237-54.

[15] W Shan. Computer analysis of foldable structures. Computers and Structures 1992;42(6):903-12.

[16] C J Gantes, *Deployable structures : Analysis and Design*, First Edition, WIT Press, Boston. 2001.

[17] C J Gantes, J J Conner, R D Logcher. Equivalent continuum model for deployable flat lattice structures. Journal of Aerospace Engineering, A S C E 1994;7:72-91.

[18] S Pellegrino, A K S Kwan, T F Van Heerden. Reduction of equilibrium, compatibility and flexibility matrices in the force method. International Journal for Numerical Methods in Engineering 1992;35:1219-36.

[19] S Pellegrino. Structural computations with the singular value decomposition of the equilibrium matrix. International Journal of Solids and Structures 1993;30(21):3025-35.

[20] A Kaveh, A Davaran. Analysis of pantograph foldable structures. Computers and Structures 1996;59:131-40.

[21] S Wolfram. *Mathematica : A System for Doing Mathematics by Computer*, Second Edition, Addition Wesley Publishing Co., 1991.

[22] C S Krishnamoorthy. *Finite Element Analysis : Theory and Programming*, Tata McGraw-Hill Publishing Company Limited, New Delhi, 1991.

APPENDIX : STIFFNESS MATRIX FOR THE SLE

The matrices $[\mathbf{J}_m]$ and $[\mathbf{J}_{mn}]$ associated with the stiffness matrix for SLE are given by

$$[\mathbf{J}_m] = \left(\begin{array}{cccccccccc} \frac{X_1-X_p}{l_1} & \frac{Y_1-Y_p}{l_1} & \frac{Z_1-Z_p}{l_1} & 0 & 0 & 0 & 0 & 0 & 0 & \\ 0 & & 0 & \frac{X_2-X_p}{l_2} & \frac{Y_2-Y_p}{l_2} & \frac{Z_2-Z_p}{l_2} & 0 & 0 & 0 & \\ 0 & 0 & 0 & 0 & 0 & 0 & \frac{X_3-X_p}{l_3} & \frac{Y_3-Y_p}{l_3} & \frac{Z_3-Z_p}{l_3} & \\ 0 & 0 & 0 & 0 & 0 & 0 & 0 & 0 & 0 & \\ & & & & 0 & 0 & 0 & \frac{X_p-X_1}{l_1} & \frac{Y_p-Y_1}{l_1} & \frac{Z_p-Z_1}{l_1} \\ & & & & 0 & 0 & 0 & \frac{X_p-X_2}{l_2} & \frac{Y_p-Y_2}{l_2} & \frac{Z_p-Z_2}{l_2} \\ & & & & 0 & 0 & 0 & \frac{X_p-X_3}{l_3} & \frac{Y_p-Y_3}{l_3} & \frac{Z_p-Z_3}{l_3} \\ & & & & \frac{X_4-X_p}{l_4} & \frac{Y_4-Y_p}{l_4} & \frac{Z_4-Z_p}{l_4} & \frac{X_p-X_4}{l_4} & \frac{Y_p-Y_4}{l_4} & \frac{Z_p-Z_4}{l_4} \end{array} \right)$$

$$[\mathbf{J}_{mn}] = \left[\begin{array}{cccccccccc} 0 & \frac{Z_p-Z_n}{l_m l_n} & \frac{Y_n-Y_p}{l_m l_n} & 0 & \frac{Z_m-Z_p}{l_m l_n} & \frac{Y_p-Y_m}{l_m l_n} & 0 & \frac{Z_n-Z_m}{l_n l_m} & \frac{Y_m-Y_n}{l_m l_n} \\ \frac{Z_n-Z_p}{l_m l_n} & 0 & \frac{X_p-X_n}{l_m l_n} & \frac{Z_p-Z_m}{l_m l_n} & 0 & \frac{X_m-X_p}{l_m l_n} & \frac{Z_m-Z_n}{l_m l_n} & 0 & \frac{X_n-X_m}{l_m l_n} \\ \frac{Y_p-Y_n}{l_m l_n} & \frac{X_n-X_p}{l_m l_n} & 0 & \frac{Y_m-Y_p}{l_m l_n} & \frac{X_p-X_m}{l_m l_n} & 0 & \frac{Y_n-Y_m}{l_m l_n} & \frac{X_m-X_n}{l_m l_n} & 0 \end{array} \right]$$